LETTER

doi:10.1038/nature13769

Programmable RNA recognition and cleavage by CRISPR/Cas9

Mitchell R. O'Connell[1], Benjamin L. Oakes[1], Samuel H. Sternberg[2], Alexandra East-Seletsky[1], Matias Kaplan[3]† & Jennifer A. Doudna[1,2,3,4]

The CRISPR-associated protein Cas9 is an RNA-guided DNA endonuclease that uses RNA–DNA complementarity to identify target sites for sequence-specific double-stranded DNA (dsDNA) cleavage[1–5]. In its native context, Cas9 acts on DNA substrates exclusively because both binding and catalysis require recognition of a short DNA sequence, known as the protospacer adjacent motif (PAM), next to and on the strand opposite the twenty-nucleotide target site in dsDNA[4–7]. Cas9 has proven to be a versatile tool for genome engineering and gene regulation in a large range of prokaryotic and eukaryotic cell types, and in whole organisms[8], but it has been thought to be incapable of targeting RNA[5]. Here we show that Cas9 binds with high affinity to single-stranded RNA (ssRNA) targets matching the Cas9-associated guide RNA sequence when the PAM is presented in *trans* as a separate DNA oligonucleotide. Furthermore, PAM-presenting oligonucleotides (PAMmers) stimulate site-specific endonucleolytic cleavage of ssRNA targets, similar to PAM-mediated stimulation of Cas9-catalysed DNA cleavage[7]. Using specially designed PAMmers, Cas9 can be specifically directed to bind or cut RNA targets while avoiding corresponding DNA sequences, and we demonstrate that this strategy enables the isolation of a specific endogenous messenger RNA from cells. These results reveal a fundamental connection between PAM binding and substrate selection by Cas9, and highlight the utility of Cas9 for programmable transcript recognition without the need for tags.

CRISPR–Cas immune systems must discriminate between self and non-self to avoid an autoimmune response[9]. In type I and II systems, foreign DNA targets that contain adjacent PAM sequences are targeted for degradation, whereas potential targets in CRISPR loci of the host do not contain PAMs and are avoided by RNA-guided interference complexes[3,5,6,10]. Single-molecule and bulk biochemical experiments showed that PAMs act both to recruit Cas9–guide-RNA (Cas9–gRNA) complexes to potential target sites and to trigger nuclease domain activation[7]. Cas9 from *Streptococcus pyogenes* recognizes a 5′-NGG-3′ PAM on the non-target (displaced) DNA strand[4,6], suggesting that PAM recognition may stimulate catalysis through allosteric regulation. Moreover, the HNH nuclease domain of Cas9, which mediates target-strand cleavage[4,5], is homologous to other HNH domains that cleave RNA substrates[11,12]. Based on the observations that single-stranded DNA (ssDNA) targets can be activated for cleavage by a separate PAMmer[7], and that similar HNH domains can cleave RNA, we wondered whether a similar strategy would enable Cas9 to cleave ssRNA targets in a programmable fashion (Fig. 1a).

Using *S. pyogenes* Cas9 and dual-guide RNAs (Methods), we performed *in vitro* cleavage experiments using a panel of RNA and DNA targets

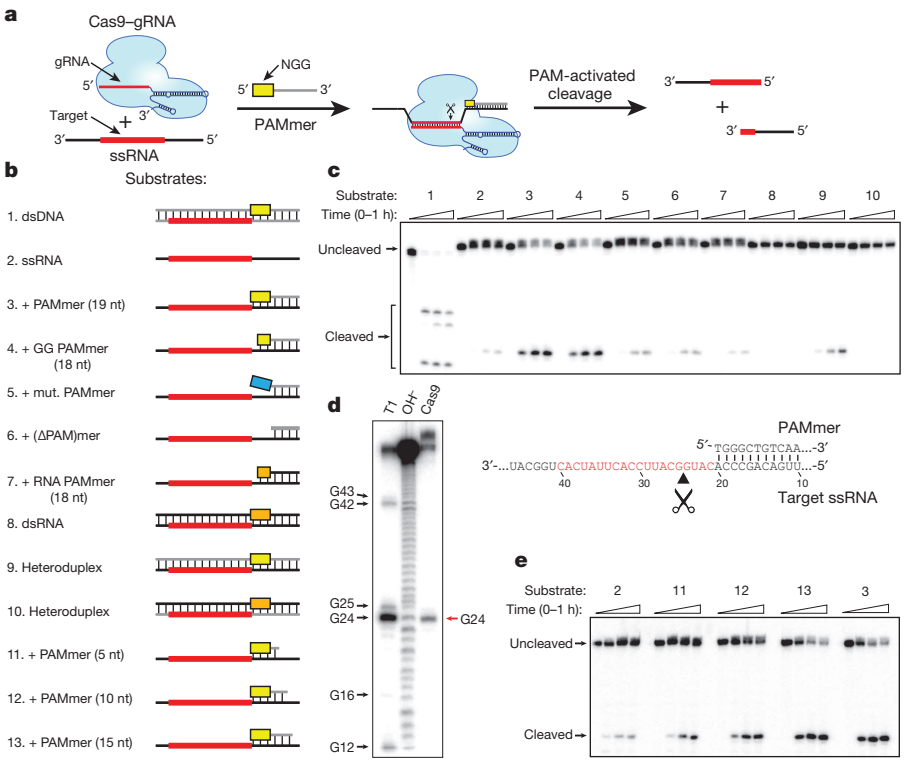


Figure 1 | RNA-guided Cas9 cleaves ssRNA targets in the presence of a short PAM-presenting DNA oligonucleotide (PAMmer). **a**, Schematic depicting the approach used to target ssRNA for programmable, sequence-specific cleavage. **b**, The panel of nucleic acid substrates examined in this study. Substrate elements are coloured as follows: DNA, grey; RNA, black; guide-RNA target sequence, red; DNA PAM, yellow; mutated DNA PAM, blue; RNA PAM, orange. The 18-nucleotide 'GG PAMmer' contains only a GG dinucleotide PAM sequence. nt, nucleotide. **c**, Representative cleavage assay for 5′-radiolabelled nucleic acid substrates using Cas9–gRNA, numbered as in **b**. **d**, Cas9–gRNA cleavage site mapping assay for substrate 3. T1 and OH^- denote RNase T1 and hydrolysis ladders, respectively; the sequence of the target ssRNA is shown at right. Sites of G cleavage by RNase T1 are shown at left. Site of Cas9 cleavage (G24) shown at right. **e**, Representative ssRNA cleavage assay in the presence of PAMmers of increasing length, numbered as in **b**.

[1]Department of Molecular and Cell Biology, University of California, Berkeley, California 94720, USA. [2]Department of Chemistry, University of California, Berkeley, California 94720, USA. [3]Howard Hughes Medical Institute, University of California, Berkeley, California 94720, USA. [4]Physical Biosciences Division, Lawrence Berkeley National Laboratory, Berkeley, California 94720, USA. †Present address: Department of Agricultural and Biological Engineering, University of Florida, Gainesville, Florida 32611, USA.

©2014 Macmillan Publishers Limited. All rights reserved

(Fig. 1b and Extended Data Table 1). Deoxyribonucleotide-comprised PAMmers specifically activated Cas9 to cleave ssRNA (Fig. 1c), an effect that required a 5′-NGG-3′ or 5′-GG-3′ PAM. RNA cleavage was not observed using ribonucleotide-based PAMmers, suggesting that Cas9 may recognize the local helical geometry and/or deoxyribose moieties within the PAM. Consistent with this hypothesis, dsRNA targets were not cleavable and RNA–DNA heteroduplexes could only be cleaved when the non-target strand was composed of deoxyribonucleotides. Notably, we found that Cas9 cleaved the ssRNA target strand between positions 4 and 5 of the base-paired gRNA–target-RNA hybrid (Fig. 1d), in contrast to the cleavage between positions 3 and 4 observed for dsDNA[3–5]. This is probably due to subtle differences in substrate positioning. However, we did observe a significant reduction in the pseudo-first-order cleavage rate constant of PAMmer-activated ssRNA as compared to ssDNA[7] (Extended Data Fig. 1).

We hypothesized that PAMmer nuclease activation would depend on the stability of the hybridized PAMmer–ssRNA duplex and tested this by varying PAMmer length. As expected, ssRNA cleavage was lost when the predicted melting temperature for the duplex decreased below the temperature used in our experiments (Fig. 1e). In addition, large molar excesses of di- or tri-deoxyribonucleotides in solution were poor activators of Cas9 cleavage (Extended Data Fig. 2). Collectively, these data demonstrate that hybrid substrate structures composed of ssRNA and deoxyribonucleotide-based PAMmers that anneal upstream of the RNA target sequence can be cleaved efficiently by RNA-guided Cas9.

We investigated the binding affinity of catalytically inactive dCas9 (Cas9 (D10A;H840A))–gRNA for ssRNA targets with and without PAMmers using a gel mobility shift assay. Notably, whereas our previous results showed that ssDNA and PAMmer-activated ssDNA targets are bound with indistinguishable affinity[7], PAMmer-activated ssRNA targets were bound >500-fold tighter than ssRNA alone (Fig. 2a, b). A recent crystal structure of Cas9 bound to a ssDNA target revealed deoxyribose-specific van der Waals interactions between the protein and the DNA backbone[13], suggesting that energetic penalties associated with ssRNA binding must be attenuated by favourable compensatory binding interactions with the provided PAM. The equilibrium dissociation constant measured for a PAMmer–ssRNA substrate was within fivefold of that for dsDNA (Fig. 2b), and this high-affinity interaction again required a cognate deoxyribonucleotide-comprised 5′-GG-3′ PAM (Fig. 2a). Tight binding also scaled with PAMmer length (Fig. 2c), consistent with the cleavage data presented above.

It is known that Cas9 possesses an intrinsic affinity for RNA, but sequence specificity of the interaction had not been explored[5]. Thus, to verify the programmable nature of PAMmer-mediated ssRNA cleavage by Cas9–gRNA, we prepared three distinct guide RNAs (λ2, λ3 and λ4; each targeting 20-nucleotide sequences within λ2, λ3 and λ4 RNAs, respectively) and showed that their corresponding ssRNA targets could be efficiently cleaved using complementary PAMmers without any detectable cross-reactivity (Fig. 3a). This result indicates that complementary RNA–RNA base pairing is critical in these reactions. Notably however, dCas9 programmed with the λ2 guide RNA bound all three PAMmer–ssRNA substrates with similar affinity (Fig. 3b). This observation suggests that high-affinity binding in this case may not require correct base pairing between the guide RNA and the ssRNA target, particularly given the compensatory role of the PAMmer.

During dsDNA targeting by Cas9–gRNA, duplex melting proceeds directionally from the PAM and strictly requires the formation of complementary RNA–DNA base pairs to offset the energetic costs associated with dsDNA unwinding[7]. We therefore wondered whether binding specificity for ssRNA substrates would be recovered using PAMmers containing 5′-extensions that create a partially double-stranded target region requiring unwinding (Fig. 3c). We found that use of a 5′-extended PAMmer enabled dCas9 bearing the λ2 guide sequence to bind sequence-selectively to the λ2 PAMmer–ssRNA target. The λ3 and λ4 PAMmer–ssRNA targets were not recognized (Fig. 3d and Extended Data Fig. 3),

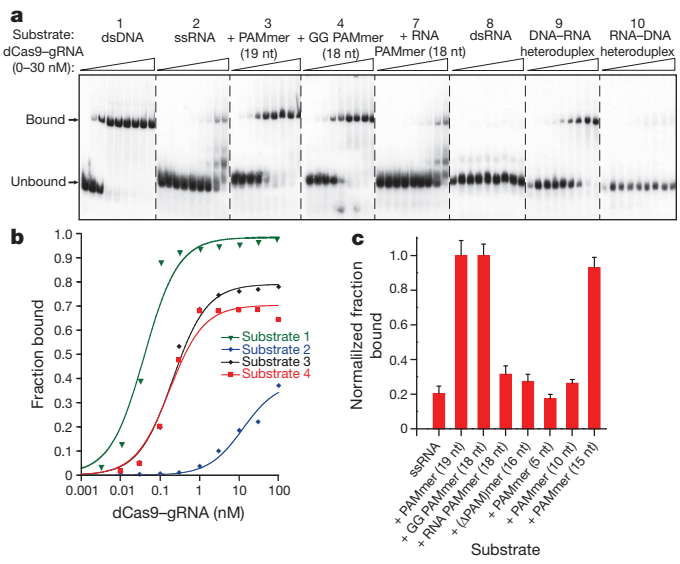


Figure 2 | dCas9–gRNA binds ssRNA targets with high affinity in the presence of PAMmers. **a**, Representative electrophoretic mobility shift assay for binding reactions with dCas9–gRNA and a panel of 5′-radiolabelled nucleic acid substrates, numbered as in Fig. 1b. **b**, Quantified binding data for substrates 1–4 from **a** fitted with standard binding isotherms. Measured dissociation constants from three independent experiments (mean ± s.d.) were 0.036 ± 0.003 nM (substrate 1), >100 nM (substrate 2), 0.20 ± 0.09 nM (substrate 3) and 0.18 ± 0.07 nM (substrate 4). **c**, Relative binding data for 1 nM dCas9–gRNA and 5′-radiolabelled ssRNA with a panel of different PAMmers. The data are normalized to the amount of binding observed at 1 nM dCas9–gRNA with a 19-nucleotide (nt) PAMmer; error bars represent the standard deviation from three independent experiments.

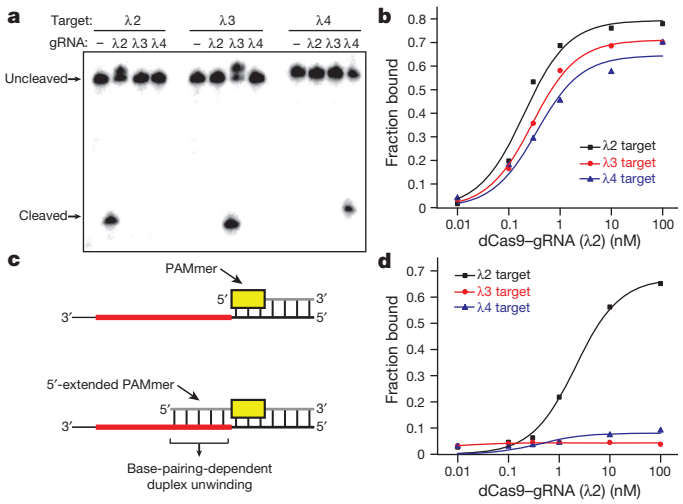


Figure 3 | 5′-extended PAMmers are required for specific target ssRNA binding. **a**, Cas9 programmed with either λ2-, λ3- or λ4-targeting gRNAs exhibits sequence-specific cleavage of 5′-radiolabelled λ2, λ3 and λ4 target ssRNAs, respectively, in the presence of cognate PAMmers. **b**, dCas9 programmed with a λ2-targeting gRNA exhibits similar binding affinity to λ2, λ3 and λ4 target ssRNAs in the presence of cognate PAMmers. Dissociation constants from three independent experiments (mean ± s.d.) were 0.20 ± 0.09 nM (λ2), 0.33 ± 0.14 nM (λ3) and 0.53 ± 0.21 nM (λ4). **c**, Schematic depicting the approach used to restore gRNA-mediated ssRNA binding specificity, which involves 5′-extensions to the PAMmer that cover part or all of the target sequence. **d**, dCas9 programmed with a λ2-targeting gRNA specifically binds the λ2 ssRNA but not λ3 and λ4 ssRNAs in the presence of complete 5′-extended PAMmers. Dissociation constants from three independent experiments (mean ± s.d.) were 3.3 ± 1.2 nM (λ2) and >100 nM (λ3 and λ4).

©2014 Macmillan Publishers Limited. All rights reserved

although we did observe a tenfold reduction in overall ssRNA substrate binding affinity. By systematically varying the length of the 5′ extension, we found that PAMmers containing 2–8 additional nucleotides upstream of the 5′-NGG-3′ offer an optimal compromise between gains in binding specificity and concomitant losses in binding affinity and cleavage efficiency (Extended Data Fig. 4).

Next we investigated whether nuclease activation by PAMmers requires base pairing between the 5′-NGG-3′ and corresponding nucleotides on the ssRNA. Prior studies have shown that DNA substrates containing a cognate PAM that is mismatched with the corresponding nucleotides on the target strand are cleaved as efficiently as a fully base-paired PAM[4]. This could enable targeting of RNA while precluding binding or cleavage of corresponding genomic DNA sites lacking PAMs (Fig. 4a). To test this possibility, we first demonstrated that Cas9–gRNA cleaves PAMmer–ssRNA substrates regardless of whether or not the PAM is base paired (Fig. 4b, c). When Cas9–RNA was incubated with both a PAMmer–ssRNA substrate and the corresponding dsDNA template containing a cognate PAM, both targets were cleaved. In contrast, when a dsDNA target lacking a PAM was incubated together with a PAMmer–ssRNA substrate bearing a mismatched 5′-NGG-3′ PAM, Cas9–gRNA selectively targeted the ssRNA for cleavage (Fig. 4c). The same result was obtained using a mismatched PAMmer with a 5′ extension (Fig. 4c), demonstrating that this general strategy enables the specific targeting of RNA transcripts while effectively eliminating any targeting of their corresponding dsDNA template loci.

We next explored whether Cas9-mediated RNA targeting could be applied in tagless transcript isolation from HeLa cells (Fig. 4d). The immobilization of Cas9 on a solid-phase resin is described in Methods (see also Extended Data Fig. 5). As a proof of concept, we first isolated *GAPDH* mRNA from HeLa total RNA using biotinylated dCas9, gRNAs and PAMmers (Extended Data Table 2) that target four non-PAM-adjacent sequences within exons 5–7 (Fig. 4e). We observed a substantial enrichment of *GAPDH* mRNA relative to control β-actin mRNA by northern blot analysis, but saw no enrichment using a non-targeting gRNA or dCas9 alone (Fig. 4f).

We then used this approach to isolate endogenous *GAPDH* transcripts from HeLa cell lysate under physiological conditions. In initial experiments, we found that Cas9–gRNA captured two *GAPDH*-specific RNA fragments rather than the full-length mRNA (Fig. 4g). Based on the sizes of these bands, we hypothesized that RNA–DNA heteroduplexes formed between the mRNA and PAMmer were cleaved by cellular RNase H. Previous studies have shown that modified DNA oligonucleotides can abrogate RNase H activity[14], and therefore we investigated whether Cas9 would tolerate chemical modifications to the PAMmer. We found that a wide range of modifications (locked nucleic acids, 2′-OMe and 2′-F ribose moieties) still enabled PAMmer-mediated nuclease

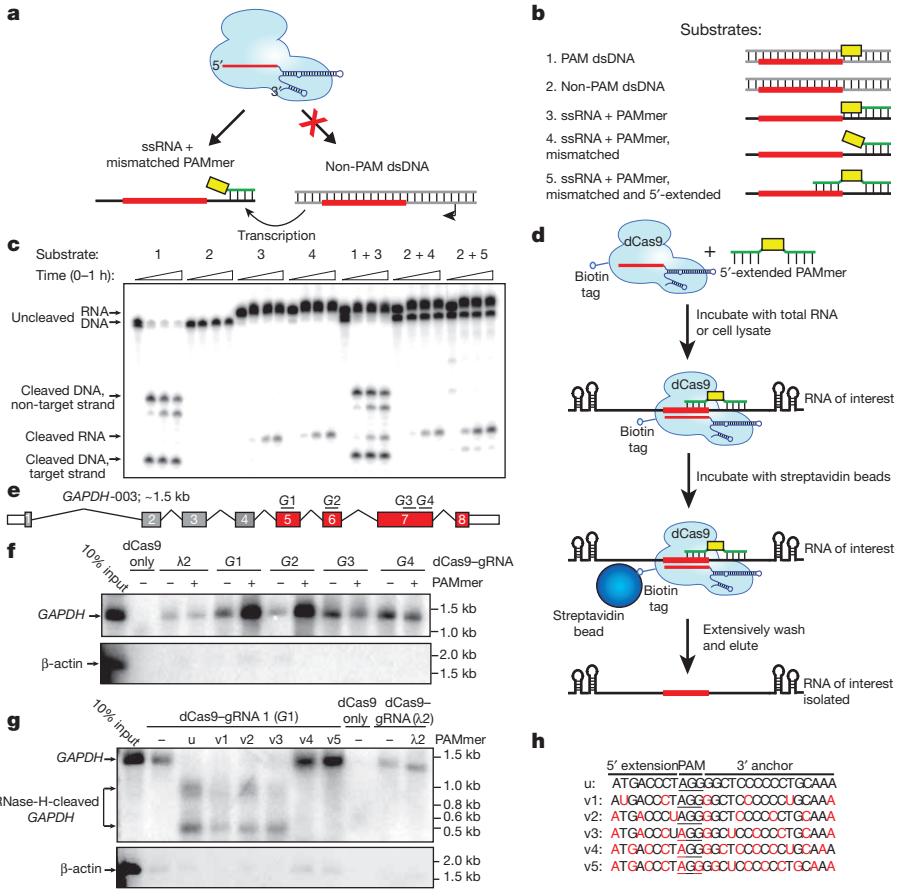


Figure 4 | RNA-guided Cas9 can target non-PAM sites on ssRNA and isolate *GAPDH* mRNA from HeLa cells in a tagless manner. **a**, Schematic of the approach designed to avoid cleavage of template DNA by targeting non-PAM sites in the ssRNA target. **b**, The panel of nucleic acid substrates tested in **c**. **c**, Cas9–gRNA cleaves ssRNA targets with equal efficiency when the 5′-NGG-3′ of the PAMmer is mismatched with the ssRNA. This strategy enables selective cleavage of ssRNA in the presence of non-PAM target dsDNA. **d**, Schematic of the dCas9 RNA pull-down experiment. **e**, *GAPDH* mRNA transcript isoform 3 (*GAPDH*-003) shown schematically, with exons common to all *GAPDH* protein-coding transcripts in red and gRNA/PAMmer targets *G1*–*G4* indicated. kb, kilobase pairs. **f**, Northern blot showing that gRNAs and corresponding 5′-extended PAMmers enable tagless isolation of *GAPDH* mRNA from HeLa total RNA; β-actin mRNA is shown as a control. **g**, Northern blot showing tagless isolation of *GAPDH* mRNA from HeLa cell lysate with varying 2′-OMe-modified PAMmers. RNase H cleavage is abrogated with v4 and v5 PAMmers; β-actin mRNA is shown as a control. u, unmodified PAMmer (*G1*). v1-v5, increasingly 2′-OMe-modified PAMmers (*G1*), see **g** for PAMmer sequences. **h**, Sequences of unmodified and modified *GAPDH* PAMmers used in **g**; 2′-OMe-modified nucleotides are shown in red.

©2014 Macmillan Publishers Limited. All rights reserved

activation (Extended Data Fig. 6). Furthermore, by varying the pattern of 2′-OMe modifications in the PAMmer, we could completely eliminate RNase-H-mediated cleavage during the pull-down and successfully isolate intact *GAPDH* mRNA (Fig. 4g, h). Notably, we consistently observed specific isolation of *GAPDH* mRNA in the absence of any PAMmer, albeit with lower efficiency, suggesting that Cas9–gRNA can bind to *GAPDH* mRNA through direct RNA–RNA hybridization (Fig. 4f, g and Extended Data Fig. 7). These experiments demonstrate that RNA-guided Cas9 can be used to purify endogenous untagged RNA transcripts. In contrast to current oligonucleotide-mediated RNA-capture methods, this approach works well under physiological salt conditions and does not require crosslinking or large sets of biotinylated probes[15–17].

Here we have demonstrated the ability to re-direct the dsDNA targeting capability of CRISPR/Cas9 for RNA-guided ssRNA binding and/or cleavage (which we now denote RCas9, an RNA-targeting Cas9). Programmable RNA recognition and cleavage has the potential to transform the study of RNA function, much as site-specific DNA targeting is changing the landscape of genetic and genomic research[8] (Extended Data Fig. 8). Although certain engineered proteins such as PPR proteins and Pumilio/FBF (PUF) repeats show promise as platforms for sequence-specific RNA targeting[18–22], these strategies require re-designing the protein for every new RNA sequence of interest. While RNA interference has proven useful for manipulating gene regulation in certain organisms[23], there has been a strong motivation to develop orthogonal nucleic-acid-based RNA recognition systems, such as the CRISPR/Cas Type III-B Cmr complex[24–28] and the atypical Cas9 from *Francisella novicida*[29,30]. In contrast to these systems, the molecular basis for RNA recognition by RCas9 is now clear and requires only the design and synthesis of a matching gRNA and complementary PAMmer. The ability to recognize endogenous RNAs within complex mixtures with high affinity and in a programmable manner paves the way for direct transcript detection, analysis and manipulation without the need for genetically encoded affinity tags.

Online Content Methods, along with any additional Extended Data display items and Source Data, are available in the online version of the paper; references unique to these sections appear only in the online paper.

Received 1 April; accepted 14 August 2014.
Published online 28 September 2014.

1. Wiedenheft, B., Sternberg, S. H. & Doudna, J. A. RNA-guided genetic silencing systems in bacteria and archaea. *Nature* **482,** 331–338 (2012).
2. Barrangou, R. *et al.* CRISPR provides acquired resistance against viruses in prokaryotes. *Science* **315,** 1709–1712 (2007).
3. Garneau, J. E. *et al.* The CRISPR/Cas bacterial immune system cleaves bacteriophage and plasmid DNA. *Nature* **468,** 67–71 (2010).
4. Jinek, M. *et al.* A programmable dual-RNA-guided DNA endonuclease in adaptive bacterial immunity. *Science* **337,** 816–821 (2012).
5. Gasiunas, G., Barrangou, R., Horvath, P. & Siksnys, V. Cas9–crRNA ribonucleoprotein complex mediates specific DNA cleavage for adaptive immunity in bacteria. *Proc. Natl Acad. Sci. USA* **109,** E2579–E2586 (2012).
6. Mojica, F. J. M., Diez-Villasenor, C., Garcia-Martinez, J. & Almendros, C. Short motif sequences determine the targets of the prokaryotic CRISPR defence system. *Microbiol* **155,** 733–740 (2009).
7. Sternberg, S. H., Redding, S., Jinek, M., Greene, E. C. & Doudna, J. A. DNA interrogation by the CRISPR RNA-guided endonuclease Cas9. *Nature* **507,** 62–67 (2014).
8. Mali, P., Esvelt, K. M. & Church, G. M. Cas9 as a versatile tool for engineering biology. *Nature Methods* **10,** 957–963 (2013).
9. Marraffini, L. A. & Sontheimer, E. J. Self versus non-self discrimination during CRISPR RNA-directed immunity. *Nature* **463,** 568–571 (2010).
10. Sashital, D. G., Wiedenheft, B. & Doudna, J. A. Mechanism of foreign DNA selection in a bacterial adaptive immune system. *Mol. Cell* **46,** 606–615 (2012).
11. Pommer, A. J. *et al.* Mechanism and cleavage specificity of the H-N-H endonuclease colicin E9. *J. Mol. Biol.* **314,** 735–749 (2001).
12. Hsia, K. C. *et al.* DNA binding and degradation by the HNH protein ColE7. *Structure* **12,** 205–214 (2004).
13. Nishimasu, H. *et al.* Crystal structure of Cas9 in complex with guide RNA and target DNA. *Cell* **156,** 935–949 (2014).
14. Wu, H. J., Lima, W. F. & Crooke, S. T. Properties of cloned and expressed human RNase H1. *J. Biol. Chem.* **274,** 28270–28278 (1999).
15. Engreitz, J. M. *et al.* The Xist lncRNA exploits three-dimensional genome architecture to spread across the X chromosome. *Science* **341** (2013).
16. Chu, C., Qu, K., Zhong, F. L., Artandi, S. E. & Chang, H. Y. Genomic maps of long noncoding RNA occupancy reveal principles of RNA–chromatin interactions. *Mol. Cell* **44,** 667–678 (2011).
17. Simon, M. D. *et al.* The genomic binding sites of a noncoding RNA. *Proc. Natl Acad. Sci. USA* **108,** 20497–20502 (2011).
18. Mackay, J. P., Font, J. & Segal, D. J. The prospects for designer single-stranded RNA-binding proteins. *Nature Struct. Mol. Biol.* **18,** 256–261 (2011).
19. Filipovska, A. & Rackham, O. Designer RNA-binding proteins: new tools for manipulating the transcriptome. *RNA Biol.* **8,** 978–983 (2011).
20. Wang, Y., Wang, Z. & Tanaka Hall, T. M. Engineered proteins with Pumilio/fem-3 mRNA binding factor scaffold to manipulate RNA metabolism. *FEBS J.* **280,** 3755–3767 (2013).
21. Yin, P. *et al.* Structural basis for the modular recognition of single-stranded RNA by PPR proteins. *Nature* **504,** 168–171 (2013).
22. Yagi, Y., Nakamura, T. & Small, I. The potential for manipulating RNA with pentatricopeptide repeat proteins. *Plant J.* **78,** 772–782 (2014).
23. Kim, D. H. & Rossi, J. J. RNAi mechanisms and applications. *Biotechniques* **44,** 613–616 (2008).
24. Hale, C. R. *et al.* RNA-guided RNA cleavage by a CRISPR RNA–Cas protein complex. *Cell* **139,** 945–956 (2009).
25. Hale, C. R. *et al.* Essential features and rational design of CRISPR RNAs that function with the Cas RAMP module complex to cleave RNAs. *Mol. Cell* **45,** 292–302 (2012).
26. Staals, R. H. J. *et al.* Structure and activity of the RNA-targeting type III-B CRISPR-Cas complex of *Thermus thermophilus*. *Mol. Cell* **52,** 135–145 (2013).
27. Spilman, M. *et al.* Structure of an RNA silencing complex of the CRISPR-Cas immune system. *Mol. Cell* **52,** 146–152 (2013).
28. Terns, R. M. & Terns, M. P. CRISPR-based technologies: prokaryotic defense weapons repurposed. *Trends Genet.* **30,** 111–118 (2014).
29. Sampson, T. R., Saroj, S. D., Llewellyn, A. C., Tzeng, Y. L. & Weiss, D. S. A. CRISPR/Cas system mediates bacterial innate immune evasion and virulence. *Nature* **497,** 254–257 (2013).
30. Sampson, T. R. & Weiss, D. S. Exploiting CRISPR/Cas systems for biotechnology. *Bioessays* **36,** 34–38 (2014).

Acknowledgements We thank B. Staahl and K. Zhou for technical assistance, A. Iavarone for assistance with mass spectrometry measurements, Integrated DNA Technologies for the synthesis of DNA and RNA oligonucleotides, and members of the Doudna laboratory and J. Cate for discussions and critical reading of the manuscript. S.H.S. acknowledges support from the National Science Foundation and National Defense Science & Engineering Graduate Research Fellowship programs. A.E.-S. and B.L.O. acknowledge support from NIH NRSA trainee grants. Funding was provided by the NIH-funded Center for RNA Systems Biology (P50GM102706-03). J.A.D. is an Investigator of the Howard Hughes Medical Institute.

Author Contributions M.R.O. and S.H.S. conceived the project. M.R.O., B.L.O., S.H.S., A.E.-S. and M.K. conducted experiments. All authors discussed the data, and M.R.O., S.H.S., B.L.O. and J.A.D. wrote the manuscript.

Author Information Reprints and permissions information is available at www.nature.com/reprints. The authors declare competing financial interests: details are available in the online version of the paper. Readers are welcome to comment on the online version of the paper. Correspondence and requests for materials should be addressed to J.A.D. (doudna@berkeley.edu).

©2014 Macmillan Publishers Limited. All rights reserved

METHODS

Cas9 and nucleic acid preparation. Wild-type Cas9 and catalytically inactive dCas9 (Cas9(D10A;H840A)) from *S. pyogenes* were purified as previously described[4]. Forty-two-nucleotide crRNAs were either ordered synthetically (Integrated DNA Technologies) or transcribed *in vitro* with T7 polymerase using single-stranded DNA templates, as described[31]. Using the previously described numbering scheme[4], tracrRNA was transcribed *in vitro* and contained nucleotides 15–87. Single-guide RNAs (sgRNAs) targeting λ-RNAs were transcribed *in vitro* from linearized plasmids and contain full-length crRNA and tracrRNA connected via a GAAA tetraloop insertion. *GAPDH* mRNA-targeting sgRNAs were transcribed *in vitro* from dsDNA PCR products based on an optimized sgRNA design[32]. Target ssRNAs (55–56 nucleotides) were transcribed *in vitro* using single-stranded DNA templates. Sequences of all nucleic acid substrates used in this study can be found in Extended Data Tables 1 and 2.

All RNAs were purified using 10–15% denaturing polyacrylamide gel electrophoresis (PAGE). Duplexes of crRNA and tracrRNA were prepared by mixing equimolar concentrations of each RNA in hybridization buffer (20 mM Tris-HCl, pH 7.5, 100 mM KCl, 5 mM $MgCl_2$), heating to 95 °C for 30 s and slow cooling. Fully double-stranded DNA/RNA substrates (substrates 1, 8–10 in Fig. 1 and substrates 1 and 2 in Fig. 4) were prepared by mixing equimolar concentrations of each nucleic acid strand in hybridization buffer, heating to 95 °C for 30 s, and slow cooling. RNA, DNA and chemically modified PAMmers were synthesized commercially (Intergrated DNA Technologies). DNA and RNA substrates were 5′-radiolabelled using [γ-^{32}P]ATP (PerkinElmer) and T4 polynucleotide kinase (New England Biolabs). Double-stranded DNA and dsRNA substrates (Figs 1c and 4c) were 5′-radiolabelled on both strands, whereas only the target ssRNA was 5′-radiolabelled in other experiments.

Cleavage assays. Cas9–gRNA complexes were reconstituted before cleavage experiments by incubating Cas9 and the crRNA–tracrRNA duplex for 10 min at 37 °C in reaction buffer (20 mM Tris-HCl, pH 7.5, 75 mM KCl, 5 mM $MgCl_2$, 1 mM dithiothreitol (DTT), 5% glycerol). Cleavage reactions were conducted at 37 °C and contained ~1 nM 5′-radiolabelled target substrate, 100 nM Cas9–RNA, and 100 nM PAMmer, where indicated. Aliquots were removed at each time point and quenched by the addition of RNA gel-loading buffer (95% deionized formamide, 0.025% (w/v) bromophenol blue, 0.025% (w/v) xylene cyanol, 50 mM EDTA (pH 8.0), 0.025% (w/v) SDS). Samples were boiled for 10 min at 95 °C before being resolved by 12% denaturing PAGE. Reaction products were visualized by phosphorimaging and quantified with ImageQuant (GE Healthcare).

RNA cleavage site mapping. A hydrolysis ladder (OH^-) was obtained by incubating ~25 nM 5′-radiolabelled λ2 target ssRNA in hydrolysis buffer (25 mM CAPS (*N*-cyclohexyl-3-aminopropanesulphonic acid), pH 10.0, 0.25 mM EDTA) at 95 °C for 10 min, before quenching on ice. An RNase T1 ladder was obtained by incubating ~25 nM 5′-radiolabelled λ2 target ssRNA with 1 U RNase T1 (New England Biolabs) for 5 min at 37 °C in RNase T1 buffer (20 mM sodium citrate, pH 5.0, 1 mM EDTA, 2 M urea, 0.1 mg ml^{-1} yeast transfer RNA). The reaction was quenched by phenol/chloroform extraction before adding RNA gel-loading buffer. All products were resolved by 15% denaturing PAGE.

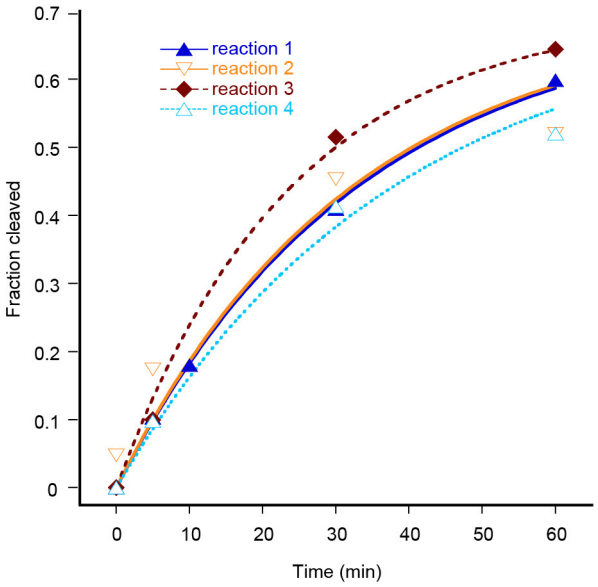
Electrophoretic mobility shift assays. In order to avoid dissociation of the Cas9–gRNA complex at low concentrations during target ssRNA binding experiments, binding reactions contained a constant excess of dCas9 (300 nM), increasing concentrations of sgRNA, and 0.1–1 nM of target ssRNA. The reaction buffer was supplemented with 10 μg ml^{-1} heparin in order to avoid non-specific association of *apo*-dCas9 with target substrates[7]. Reactions were incubated at 37 °C for 45 min before being resolved by 8% native PAGE at 4 °C (0.5 × TBE buffer with 5 mM $MgCl_2$). RNA and DNA were visualized by phosphorimaging, quantified with ImageQuant (GE Healthcare), and analysed with Kaleidagraph (Synergy Software).

Cas9 biotin labelling. To ensure specific labelling at a single residue on Cas9, two naturally occurring cysteine residues were mutated to serine (C80S and C574S) and a cysteine point mutant was introduced at residue Met 1. To attach the biotin moiety, 10 μM wild-type Cas9 or dCas9 was reacted with a 50-fold molar excess of EZ-Link Maleimide-PEG2-Biotin (Thermo Scientific) at 25 °C for 2 h. The reaction was quenched by the addition of 10 mM DTT, and unreacted Maleimide-PEG2-Biotin was removed using a Bio-Gel P-6 column (Bio-Rad). Labelling was verified using a streptavidin bead binding assay, where 8.5 pmol of biotinylated Cas9 or non-biotinylated Cas9 was mixed with either 25 μl streptavidin-agarose (Pierce Avidin Agarose; Thermo Scientific) or 25 μl streptavidin magnetic beads (Dynabeads MyOne Streptavidin C1; Life Technologies). Samples were incubated in Cas9 reaction buffer at room temperature for 30 min, followed by three washes with Cas9 reaction buffer and elution in boiling SDS–PAGE loading buffer. Elutions were analysed using SDS–PAGE. Cas9 M1C biotinylation was also confirmed using mass spectroscopy performed in the QB3/Chemistry Mass Spectrometry Facility at UC Berkeley. Samples of intact Cas9 proteins were analysed using an Agilent 1200 liquid chromatograph equipped with a Viva C8 (100 mm × 1.0 mm, 5 μm particles, Restek) analytical column and connected in-line with an LTQ Orbitrap XL mass spectrometer (Thermo Fisher Scientific). Mass spectra were recorded in the positive ion mode. Mass spectral deconvolution was performed using ProMass software (Novatia).

***GAPDH* mRNA pull-down.** HeLa-S3 cell lysates were prepared as previously described[33]. Total RNA was isolated from HeLa-S3 cells using Trizol reagent according to the manufacturer's instructions (Life Technologies). Cas9–sgRNA complexes were reconstituted before pull-down experiments by incubating a twofold molar excess of Cas9 with sgRNA for 10 min at 37 °C in reaction buffer. HeLa total RNA (40 μg) or HeLa lysate (~5×10^6 cells) was added to reaction buffer with 40 U RNasin (Promega), PAMmer (5 μM) and the biotin-dCas9 (50 nM)–sgRNA (25 nM) in a total volume of 100 μl and incubated at 37 °C for 1 h. This mixture was then added to 25 μl magnetic streptavidin beads (Dynabeads MyOne Streptavidin C1; Life Technologies) pre-equilibrated in reaction buffer and agitated at 4 °C for 2 h. Beads were then washed six times with 300 μl wash buffer (20 mM Tris-HCl, pH 7.5, 150 mM NaCl, 5 mM $MgCl_2$, 0.1% Triton X-100, 5% glycerol, 1 mM DTT, 10 μg ml^{-1} heparin). Immobilized RNA was eluted by heating beads at 70 °C in the presence of DEPC-treated water and a phenol/chloroform mixture. Eluates were then treated with an equal volume of glyoxal loading dye (Life Technologies) and heated at 50 °C for 1 h before separation via 1% BPTE agarose gel (30 mM Bis-Tris, 10 mM PIPES, 10 mM EDTA, pH 6.5). Northern blot transfers were carried out as previously described[34]. Following transfer, membranes were crosslinked using UV radiation and incubated in pre-hybridization buffer (UltraHYB Ultrasensitive Hybridization Buffer; Life Technologies) for 1 h at 46 °C before hybridization. Radioactive northern probes were synthesized using random priming of *GAPDH* and β-actin partial cDNAs (for cDNA primers, see Extended Data Table 2) in the presence of [α-^{32}P]dATP (PerkinElmer), using a Prime-It II Random Primer Labelling kit (Agilent Technologies). Hybridization was carried out for 3 h in pre-hybridization buffer at 46 °C followed by two washes with 2 × SSC (300 mM NaCl, 30 mM trisodium citrate, pH 7, 0.5% (w/v) SDS) for 15 min at 46 °C. Membranes were imaged using a phosphorscreen.

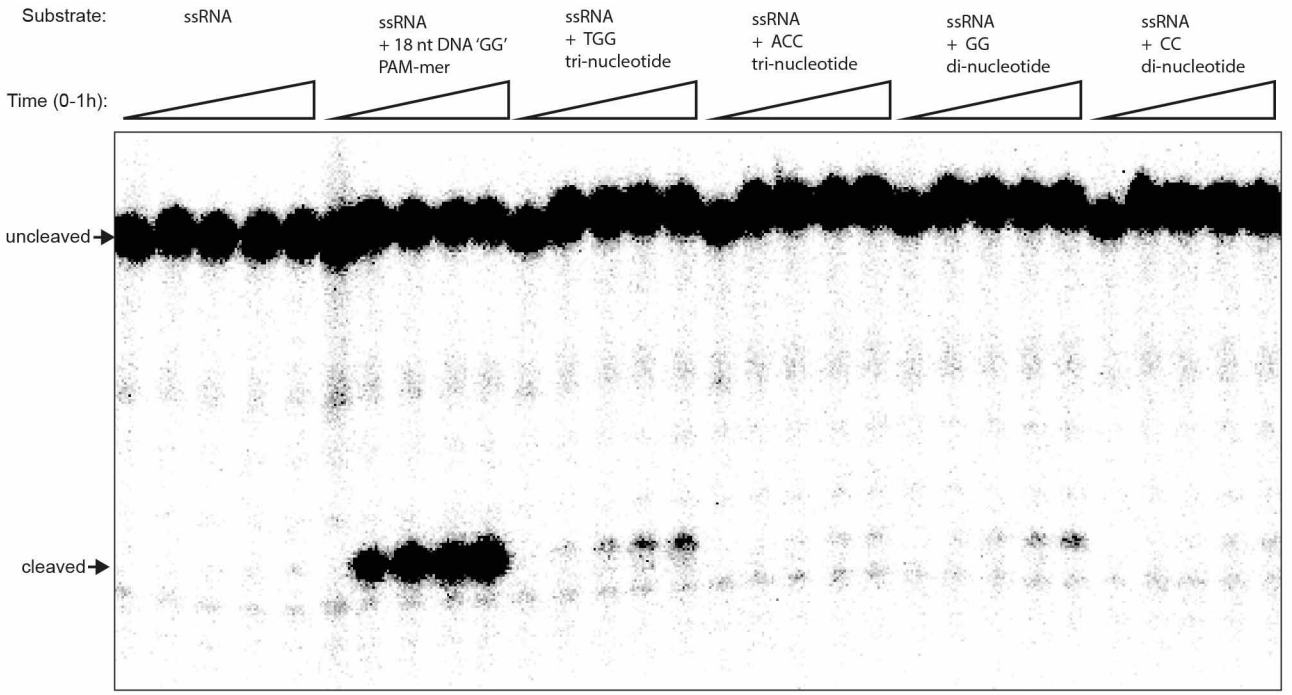
31. Sternberg, S. H., Haurwitz, R. E. & Doudna, J. A. Mechanism of substrate selection by a highly specific CRISPR endoribonuclease. *RNA* **18,** 661–672 (2012).
32. Chen, B. *et al.* Dynamic imaging of genomic loci in living human cells by an optimized CRISPR/Cas system. *Cell* **155,** 1479–1491 (2013).
33. Lee, H. Y. *et al.* RNA-protein analysis using a conditional CRISPR nuclease. *Proc. Natl Acad. Sci. USA* **110,** 5416–5421 (2013).
34. Chomczynski, P. One-hour downward alkaline capillary transfer for blotting of DNA and RNA. *Anal. Biochem.* **201,** 134–139 (1992).

©2014 Macmillan Publishers Limited. All rights reserved



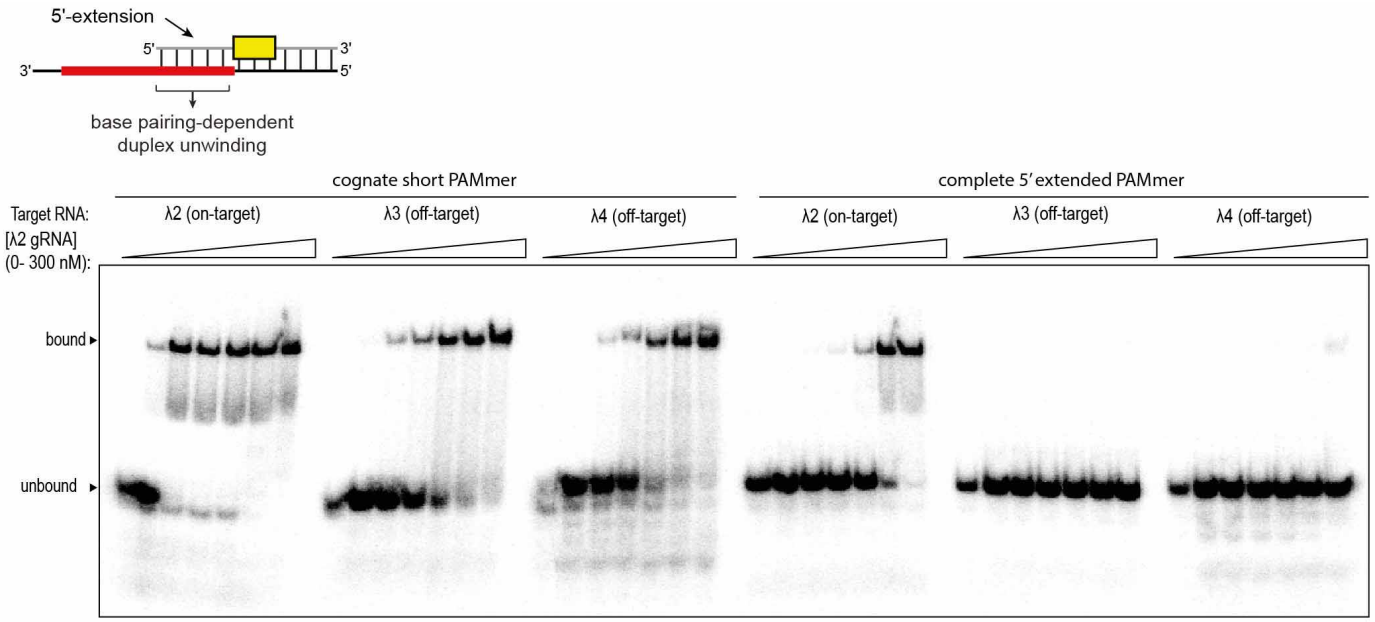
Extended Data Figure 1 | Quantified data for cleavage of ssRNA by Cas9–gRNA in the presence of a 19-nucleotide PAMmer. Cleavage assays were conducted as described in the Methods, and the quantified data were fitted with single-exponential decays. Results from four independent experiments yielded an average apparent pseudo-first-order cleavage rate constant (mean ± s.d.) of $0.032 \pm 0.007\ min^{-1}$. This is slower than the rate constant determined previously for ssDNA in the presence of the same 19-nucleotide PAMmer ($7.3 \pm 3.2\ min^{-1}$)[7].

©2014 Macmillan Publishers Limited. All rights reserved



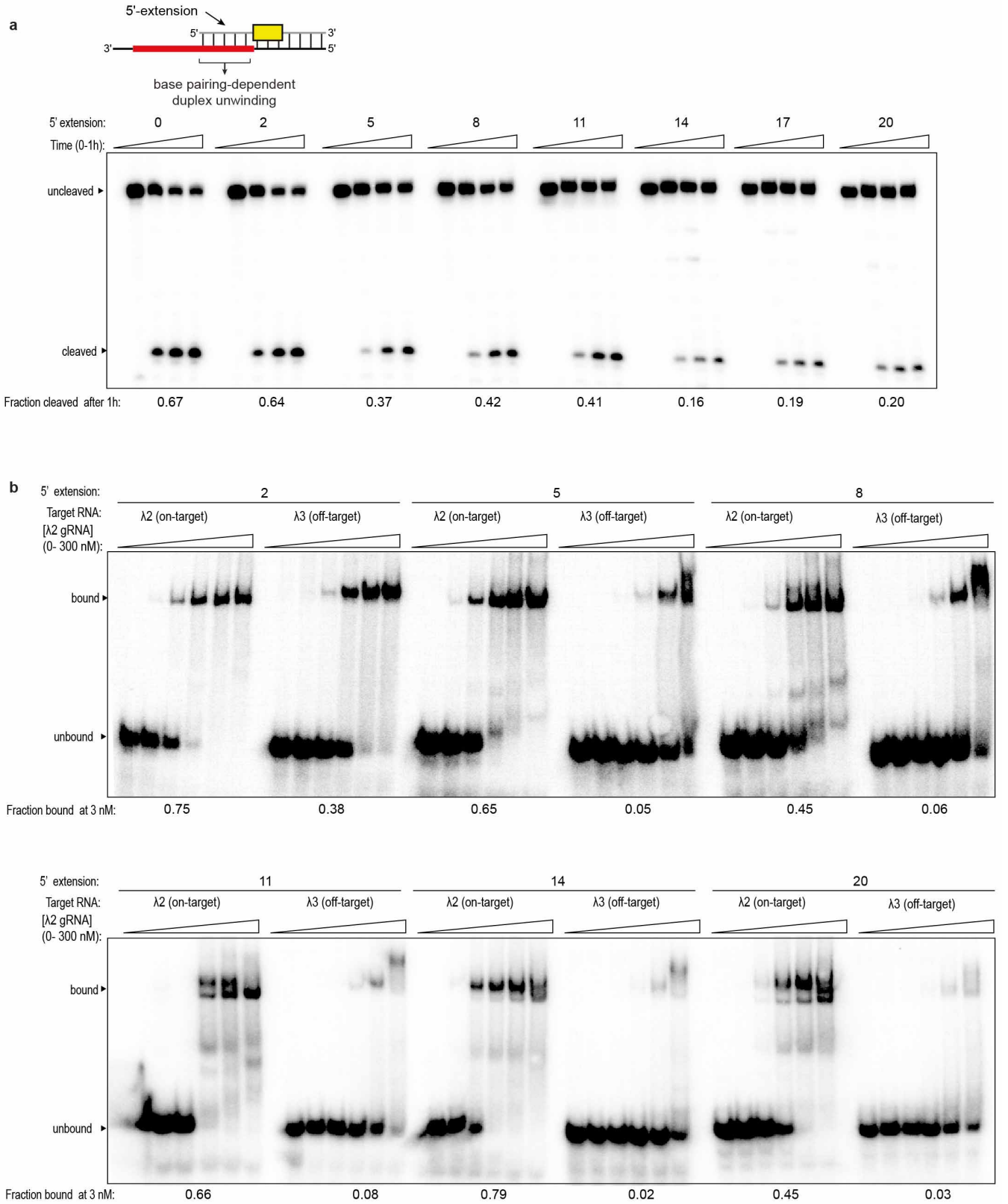
Extended Data Figure 2 | RNA cleavage is marginally stimulated by di- and tri-deoxyribonucleotide PAMmers. Cleavage reactions contained ~1 nM 5′-radiolabelled target ssRNA and no PAMmer (left), 100 nM 18-nt PAMmer (second from left), or 1 mM of the indicated di- or tri-nucleotide (remaining lanes). Reaction products were resolved by 12% denaturing polyacrylamide gel electrophoresis (PAGE) and visualized by phosphorimaging.

©2014 Macmillan Publishers Limited. All rights reserved



Extended Data Figure 3 | Representative binding experiment demonstrating guide-specific ssRNA binding with 5′-extended PAMmers. Gel shift assays were conducted as described in the Methods. Binding reactions contained Cas9 programmed with λ2 gRNA and either λ2 (on-target), λ3 (off-target) or λ4 (off-target) ssRNA in the presence of short cognate PAMmers or cognate PAMmers with complete 5′-extensions, as indicated. The presence of a cognate 5′-extended PAM-mer abrogates off-target binding. Three independent experiments were conducted to produce the data shown in Fig. 3b, d.

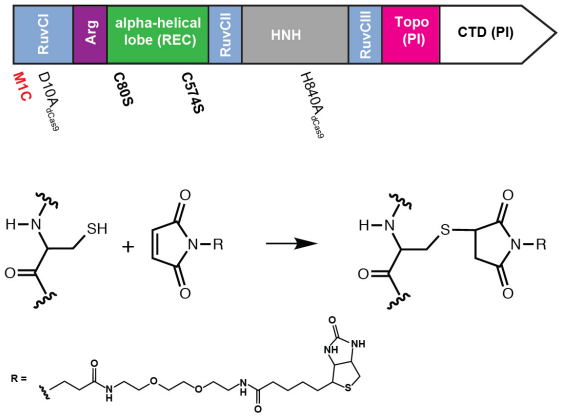
©2014 Macmillan Publishers Limited. All rights reserved



Extended Data Figure 4 | Exploration of RNA cleavage efficiencies and binding specificity using PAMmers with variable 5′-extensions. **a**, Cleavage assays were conducted as described in Methods. Reactions contained Cas9 programmed with λ2 gRNA and λ2 ssRNA targets in the presence of PAMmers with 5′-extensions of variable length. The ssRNA cleavage efficiency decreases as the PAMmer extends further into the target region, as indicated by the fraction of RNA cleaved after 1 h. **b**, Binding assays were conducted as described in the Methods, using mostly the same panel of 5′-extended PAMmers as in **a**. Binding reactions contained Cas9 programmed with λ2 gRNA and either λ2 (on-target) or λ3 (off-target) ssRNA in the presence of cognate PAMmers with 5′-extensions of variable length. The binding specificity increases as the PAMmer extends further into the target region, as indicated by the fraction of λ3 (off-target) ssRNA bound at 3 nM Cas9–gRNA. PAMmers with 5′ extensions also cause a slight reduction in the relative binding affinity of λ2 (on-target) ssRNA.

©2014 Macmillan Publishers Limited. All rights reserved

a

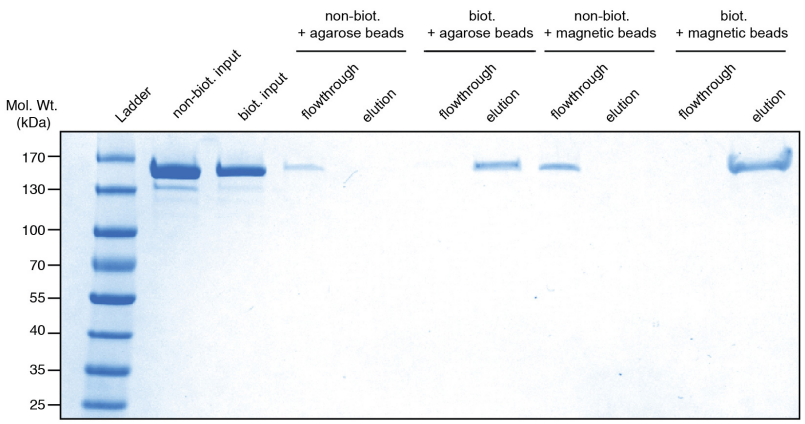


b

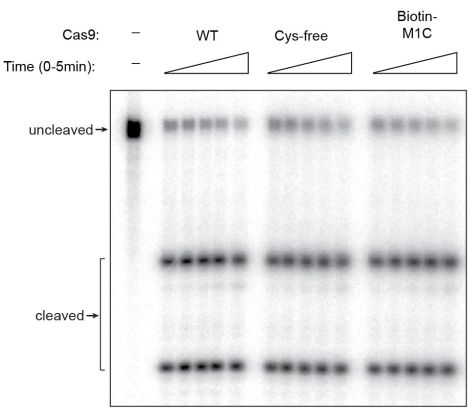
Mass Spectroscopy Data

Cas9 Mutant	Predicted Mass (Da)	Unlabeled Mass (Da)	Labeled Mass (Da)	ΔLabel (Da)
Cys-Free	158,681.5	158,681	158,681	0
M1C	158,653.5	158,653	159,179	527

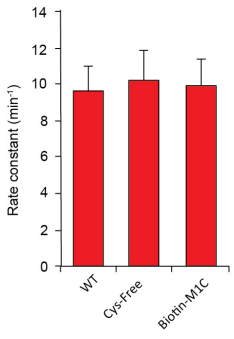
c



d

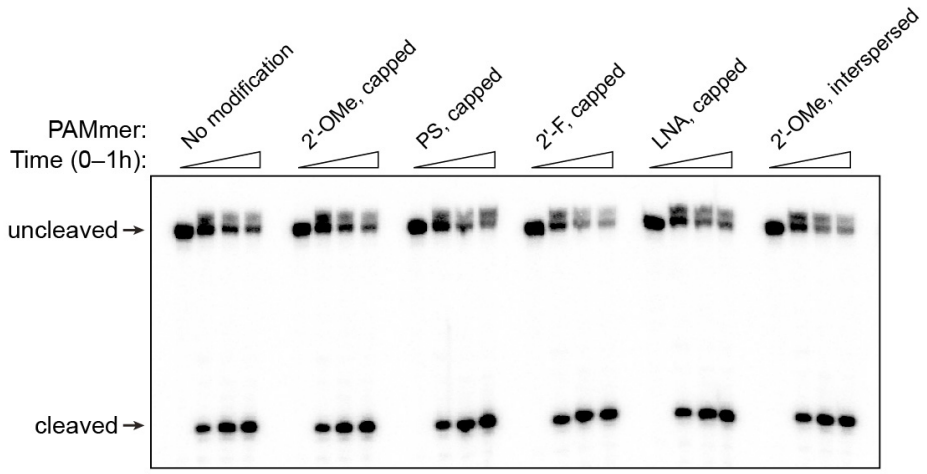


e



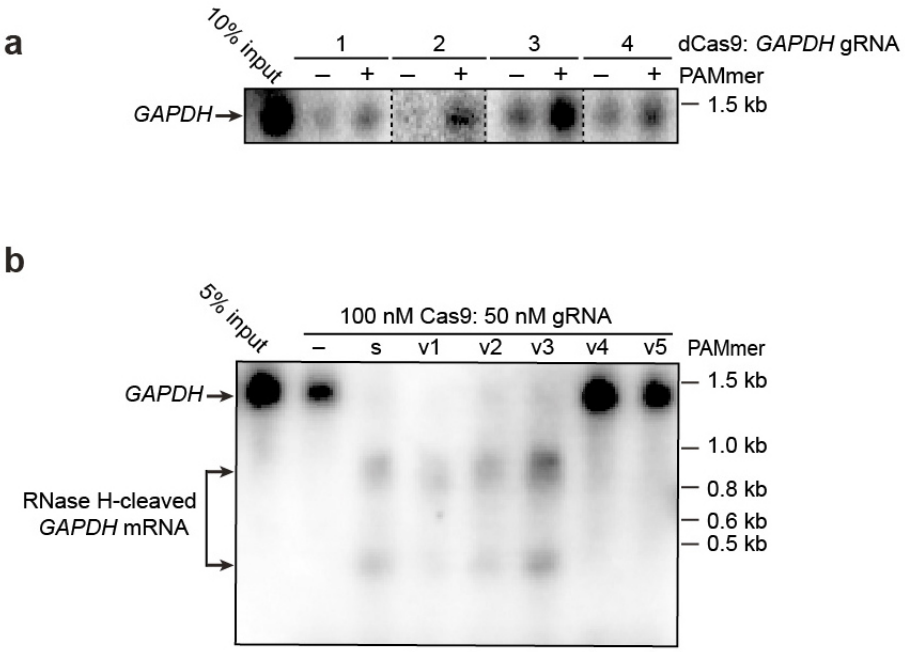
Extended Data Figure 5 | Site-specific biotin labelling of Cas9. **a**, In order to introduce a single biotin moiety on Cas9, the solvent accessible, non-conserved amino-terminal methionine was mutated to a cysteine (M1C; red text) and the naturally occurring cysteine residues were mutated to serine (C80S and C574S; bold text). This enabled cysteine-specific labelling with EZ-link Maleimide-PEG2-biotin through an irreversible reaction between the reduced sulphydryl group of the cysteine and the maleimide group present on the biotin label. Mutations of dCas9 are also indicated in the domain schematic. **b**, Mass spectrometry analysis of the Cas9 biotin-labelling reaction confirmed that successful biotin labelling only occurs when the M1C mutation is present in the Cys-free background (C80S;C574S). The mass of the Maleimide-PEG2-biotin reagent is 525.6 Da. **c**, Streptavidin bead binding assay with biotinylated (biot.) or non-biotinylated (non-biot.) Cas9 and streptavidin agarose or streptavidin magnetic beads. Cas9 only remains specifically bound to the beads after biotin labelling. **d**, Cleavage assays were conducted as described in the Methods and resolved by denaturing PAGE. Reactions contained 100 nM Cas9 programmed with λ2 gRNA and ~1 nM 5′-radiolabelled λ2 dsDNA target. **e**, Quantified cleavage data from triplicate experiments were fitted with single-exponential decays to calculate the apparent pseudo-first-order cleavage rate constants (average ± standard deviation). Both Cys-free and biotin-labelled Cas9(M1C) retain wild-type activity.

©2014 Macmillan Publishers Limited. All rights reserved



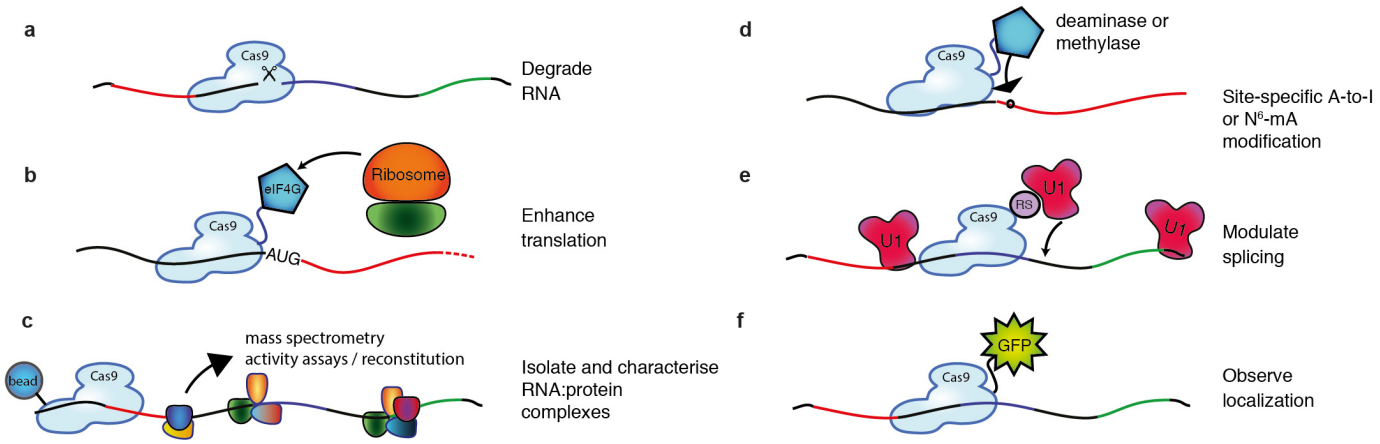
Extended Data Figure 6 | RNA-guided Cas9 can utilize chemically modified PAMmers. Nineteen-nucleotide PAMmer derivatives containing various chemical modifications on the 5′ and 3′ ends (capped) or interspersed throughout the strand still activate Cas9 for cleavage of ssRNA targets. These types of modification are often used to increase the *in vivo* half-life of short oligonucleotides by preventing exo- and endonuclease-mediated degradation. Cleavage assays were conducted as described in the Methods. PS, phosphorothioate bonds; LNA, locked nucleic acid.

©2014 Macmillan Publishers Limited. All rights reserved



Extended Data Figure 7 | Cas9 programmed with *GAPDH*-specific gRNAs can pull down *GAPDH* mRNA in the absence of PAMmers. a, Northern blot showing that, in some cases, Cas9–gRNA is able to pull down detectable amounts of *GAPDH* mRNA from total RNA without requiring a PAMmer. **b**, Northern blot showing that Cas9–gRNA *G*1 is also able to pull down quantitative amounts of *GAPDH* mRNA from HeLa cell lysate without requiring a PAMmer. s, standard; v1-5, increasingly 2′-OMe-modified PAMmers. See Fig. 4g for PAMmer sequences.

©2014 Macmillan Publishers Limited. All rights reserved



Extended Data Figure 8 | Potential applications of RCas9 for untagged transcript analysis, detection and manipulation. **a**, Catalytically active RCas9 could be used to target and cleave RNA, particularly those for which RNA-interference-mediated repression/degradation is not possible. **b**, Tethering the eukaryotic initiation factor eIF4G to a catalytically inactive dRCas9 targeted to the 5′ untranslated region of an mRNA could drive translation. **c**, dRCas9 tethered to beads could be used to specifically isolate RNA or native RNA–protein complexes of interest from cells for downstream analysis or assays including identification of bound-protein complexes, probing of RNA structure under native protein-bound conditions, and enrichment of rare transcripts for sequencing analysis. **d**, dRCas9 tethered to RNA deaminase or N6-mA methylase domains could direct site-specific A-to-I editing or methylation of RNA, respectively. **e**, dRCas9 fused to a U1 recruitment domain (arginine- and serine-rich (RS) domain) could be programmed to recognize a splicing enhancer site and thereby promote the inclusion of a targeted exon. **f**, dRCas9 tethered to a fluorescent protein such as GFP could be used to observe RNA localization and transport in living cells. Adapted from Mackay *et al.*[18]

©2014 Macmillan Publishers Limited. All rights reserved

Extended Data Table 1 | λ-Oligonucleotide sequences

Description	Sequence *	Used in
Oligo for T7 promoter, in vitro transcription	5′-**TAATACGACTCACTATA**-3′	NA
λ2-targeting crRNA	5′-GUGAUAAGUGGAAUGCCAUGGUUUUAGAGCUAUGCUGUUUUG-3′	Fig. 1c-e, 3a, 4c-d, ED1-2, 4a
λ3-targeting crRNA	5′-CUGGUGAACUUCCGAUAGUGGUUUUAGAGCUAUGCUGUUUUG-3′	Fig. 3a
λ4-targeting crRNA	5′-CAGATATAGCCTGGTGGTTCGUUUUAGAGCUAUGCUGUUUUG-3′	Fig. 3a
ssDNA T7 template†, tracrRNA	5′-AAAAAGCACCGACTCGGTGCCACTTTTTCAAGTTGATAACGGACTAGCCTTATTTTAACTTGCTATGCTGT**CCTA TAGTGAGTCGTATTA**-3′	NA
tracrRNA (nt 15-87)	5′-GGACAGCAUAGCAAGUUAAAAUAAGGCUAGUCCGUUAUCAACUUGAAAAAGUGGCACCGAGUCGGUGCUUUUU-3′	Fig. 1c-e, 3a, 4c-d, ED1-2,4a
λ2-targeting sgRNA T7 template‡	5′-**TAATACGACTCACTATAGG**TGATAAGTGGAATGCCATGGTTTTAGAGCTATGCTGTTTTGGAAACAAAACAGCATA GCAAGTTAAAATAAGGCTAGTCCGTTATCAACTTGAAAAAGTGGCACCGAGTCGGTGCTTTTTTT-3′	NA
λ2-targeting sgRNA	5′-**GG**UGAUAAGUGGAAUGCCAUGGUUUUAGAGCUAUGCUGUUUUGGAAACAAAACAGCAUAGCAAGUUAAAAUAAGGC UAGUCCGUUAUCAACUUGAAAAAGUGGCACCGAGUCGGUGCUUUUUUU-3′	Fig 2, 3b,d, ED3, 4b
λ2 target dsDNA duplex	5′-GAGTGGAAGGATGCCAGTGATAAGTGGAATGCCATG**TGG**GCTGTCAAAATTGAGC-3′ 3′-CTCACCTTCCTACGGT**CACTATTCACCTTACGGTAC**ACCCGACAGTTTTAACTCG-5′	Fig. 1c, 2a, 4c
λ2 ssDNA target strand (used to make heteroduplex DNA:RNA)	3′-CTCACCTTCCTACGGT**CACTATTCACCTTACGGTAC**ACCCGACAGTTTTAACTCG-5′	Fig. 1c, 2a
λ2 ssDNA non-target strand (used to make heteroduplex DNA:RNA)	5′-GAGTGGAAGGATGCCAGTGATAAGTGGAATGCCATG**TGG**GCTGTCAAAATTGAGC-3′	Fig 1c, 2a, 3d, ED3
λ2 ssRNA target strand T7 template	5′-GAGTGGAAGGATGCCAGTGATAAGTGGAATGCCATGTGGGCTGTCAAAATTGAGC**CTATAGTGAGTCGTATTA**-3′	NA
λ2 ssRNA target strand	3′-CUCACCUUCCUACGGU**CACUAUUCACCUUACGGUAC**ACCCGACAGUUUUAACUCG**G**-5′	Fig. 1c-e, 2, 3, 4, ED1-4
λ2 ssRNA non-target strand T7 template	5′-GCTCAATTTTGACAGCCCACATGGCATTCCACTTATCACTGGCATCCTTCCACTCC**TATAGTGAGTCGTATTA**-3′	NA
λ2 ssRNA non-target strand (used to make dsRNA)	5′-**G**GAGTGGAAGGATGCCAGTGATAAGTGGAATGCCATG**TGG**GCTGTCAAAATTGAGC-3′	Fig. 1c, 2a
19 nt λ2 DNA PAMmer	5′-**TGG**GCTGTCAAAATTGAGC-3′	Fig. 1c-e, 2, 3a-b, ED 1-4
18 nt λ2 "GG" DNA PAMmer	5′-**GG**GCTGTCAAAATTGAGC-3′	Fig. 1c, 2
19 nt λ2 DNA mutated PAMmer	5′-ACCGCTGTCAAAATTGAGC-3′	Fig. 1c, 2c
16 nt λ2 DNA "PAM-less" PAMmer	5′-GCTGTCAAAATTGAGC-3′	Fig. 1c, 2c
18 nt λ2 RNA PAMmer	5′-**GG**GCUGUCAAAAUUGAGC-3′	Fig. 1c, 2a
5 nt λ2 DNA PAMmer	5′-**TGG**GC-3′	Fig. 1e, 2c
10 nt λ2 DNA PAMmer	5′-**TGG**GCTGTCA-3′	Fig. 1e, 2c
15 nt λ2 DNA PAMmer	5′-**TGG**GCTGTCAAAATT-3′	Fig. 1e, 2c
λ3 ssRNA target strand T7 template	5′-AACGTGCTGCGGCTGGCTGGTGAACTTCCGATAGTGCGGGTGTTGAATGATTTCC**TATAGTGAGTCGTATTA**-3′	NA
λ3 ssRNA target strand	3′-UUGCACGACGCCGACC**GACCACUUGAAGGCUAUCAC**GCCCACAACUUACUAAAGG-5′	Fig. 3a,b,d, ED3, 4b
λ4 ssRNA target strand T7 template	5′-TCACAACAATGAGTGGCAGATATAGCCTGGTGGTTCAGGCGGCGCATTTTTATTGC**CTATAGTGAGTCGTATTA**-3′	NA
λ4 ssRNA target strand	3′-AGUGUUGUUACUCACC**GUCUAUAUCGGACCACCAAG**UCCGCCGCGUAAAAAUAAC**GG**-5′	Fig. 3a,b,d, ED3
λ3 ssDNA non-target strand	5′-AACGTGCTGCGGCTGGCTGGTGAACTTCCGATAGTG**CGG**GTGTTGAATGATTTCC-3′	Fig. 3d, ED3
λ4 ssDNA non-target strand	5′-TCACAACAATGAGTGGCAGATATAGCCTGGTGGTTC**AGG**CGGCGCATTTTTATTG-3′	Fig. 3d, ED3
19 nt λ3 DNA PAMmer	5′-**CGG**GTGTTGAATGATTTCC-3′	Fig. 3a,b,d, ED3, 4
19 nt λ4 DNA PAMmer	5′-**AGG**CGGCGCATTTTTATTG-3′	Fig. 3a,b,d, ED3
21 nt λ2 5′-extended DNA PAMmer	5′-TG**TGG**GCTGTCAAAATTGAGC-3′	Fig. 4c, ED 4a,b
21 nt λ3 5′-extended DNA PAMmer	5′-TG**CGG**GTGTTGAATGATTTCC-3′	ED 4b
24 nt λ2 5′-extended DNA PAMmer	5′-CCATG**TGG**GCTGTCAAAATTGAGC-3′	ED 4a,b
24 nt λ3 5′-extended DNA PAMmer	5′-TAGTG**CGG**GTGTTGAATGATTTCC-3′	ED 4b
27 nt λ2 5′-extended DNA PAMmer	5′-ATGCCATG**TGG**GCTGTCAAAATTGAGC-3′	Fig. 4f,g, ED 4a,b
27 nt λ3 5′-extended DNA PAMmer	5′-CGATAGTG**CGG**GTGTTGAATGATTTCC-3′	ED 4b
30 nt λ2 5′-extended DNA PAMmer	5′-GGAATGCCATG**TGG**GCTGTCAAAATTGAGC-3′	ED 4a,b
30 nt λ3 5′-extended DNA PAMmer	5′-TTCCGATAGTG**CGG**GTGTTGAATGATTTCC-3′	ED 4b
33 nt λ2 5′-extended DNA PAMmer	5′-AGTGGAATGCCATG**TGG**GCTGTCAAAATTGAGC-3′	ED 4a,4b
33 nt λ3 5′-extended DNA PAMmer	5′-AACTTCCGATAGTG**CGG**GTGTTGAATGATTTCC-3′	ED 4b
36 nt λ2 5′-extended DNA PAMmer	5′-ATAAGTGGAATGCCATG**TGG**GCTGTCAAAATTGAGC-3′	ED 4a
39 nt λ2 5′-extended DNA PAMmer	5′-GTGATAAGTGGAATGCCATG**TGG**GCTGTCAAAATTGAGC-3′	ED 4a,4b
39 nt λ3 5′-extended DNA PAMmer	5′-CTGGTGAACTTCCGATAGTG**CGG**GTGTTGAATGATTTCC-3′	Fig. 4b
non-PAM λ2 dsDNA	5′-GAGTGGAAGGATGCCAGTGATAAGTGGAATGCCATG**ACG**GCTGTCAAAATTGAGC-3′ 3′-CTCACCTTCCTACGGT**CACTATTCACCTTACGGTAC**TGGCGACAGTTTTAACTCG-5′	Fig. 4c
non-PAM λ2 ssRNA target strand T7 template	5′-GAGTGGAAGGATGCCAGTGATAAGTGGAATGCCATGACCGGCTGTCAAAATTGAG**CCTATAGTGAGTCGTATTA**-3′	NA
non-PAM λ2 ssRNA target strand	3′-CUCACCUUCCUACGGU**CACUAUUCACCUUACGGUAC**TGGCGACAGUUUUAACUC**GG**-5′	Fig. 4c
λ2 2′OMe capped PAMmer§	5′-*U**GG**GCUGUCAAAAUUGAG*C-3′	ED 6
λ2 PS capped PAMmer§	5′-**T*GG**GCTGTCAAAATTGAG*C-3′	ED 6
λ2 2′F capped PAMmer§	5′-*U**GG**GCUGUCAAAAUUGAG*C-3′	ED 6
λ2 LNA capped PAMmer§	5′-*T**GG**GCTGTCAAAATTGAG*C-3′	ED 6
λ2 19 nt 2′OMe interspersed PAMmer§	5′-*U**GG**G*CUGUC*AAAAUU*GAG*C-3′	ED 6

* Guide crRNA sequences and complementary DNA target strand sequences are shown in red. PAM sites (5′-NGG-3′) are highlighted in yellow on the non-target strand when adjacent to the target sequence or in the PAMmer.
† The T7 promoter is indicated in bold (or reverse complement of), as well as 5′ G or GG included in the ssRNA product by T7 polymerase.
‡ sgRNA template obtained from pIDT, subsequently linearized by AflII for run-off transcription.
§ Positions of modifications depicted with asterisks preceding each modified nucleotide in each case (except for PS linkages which are depicted between bases).
PS, phosphorothioate bond; NA, not applicable; LNA, locked nucleic acid.

©2014 **Macmillan Publishers Limited. All rights reserved**

Extended Data Table 2 | Oligonucleotides used in the *GAPDH* mRNA pull-down experiment

Description	Sequence *	Used in
GAPDH-targeting sgRNA 1 T7 template†	5′-**TAATACGACTCACTATA**GGGGCAGAGATGATGACCCTGTTTAAGAGCTATGCTGGAAACAGCATAGCAAGTTTAAATAA GGCTAGTCCGTTATCAACTTGAAAAAGTGGCACCGAGTCGGTGCTTTTTTT-3′	NA
GAPDH-targeting sgRNA 1	5′-GGGGCAGAGATGATGACCCTGTTTAAGAGCTATGCTGGAAACAGCATAGCAAGTTTAAATAAGGCTAGTCCGTTATCAAC TTGAAAAAGTGGCACCGAGTCGGTGCTTTTTTT-3′	Fig. 4f,g, ED 7
GAPDH-targeting sgRNA 2 T7 template†	5′-**TAATACGACTCACTATAGG**CCAAAGTTGTCATGGATGACGTTTAAGAGCTATGCTGGAAACAGCATAGCAAGTTTAAAT AAGGCTAGTCCGTTATCAACTTGAAAAAGTGGCACCGAGTCGGTGCTTTTTTT-3′	NA
GAPDH-targeting sgRNA 2	5′-**GG**CCAAAGTTGTCATGGATGACGTTTAAGAGCTATGCTGGAAACAGCATAGCAAGTTTAAATAAGGCTAGTCCGTTATCA ACTTGAAAAAGTGGCACCGAGTCGGTGCTTTTTTT-3′	Fig. 4f, ED 7
GAPDH-targeting sgRNA 3 T7 template†	5′-**TAATACGACTCACTATAGG**CCAAAGTTGTCATGGATGACGTTTAAGAGCTATGCTGGAAACAGCATAGCAAGTTTAAAT AAGGCTAGTCCGTTATCAACTTGAAAAAGTGGCACCGAGTCGGTGCTTTTTTT-3′	NA
GAPDH-targeting sgRNA 3	5′-**GG**CCAAAGTTGTCATGGATGACGTTTAAGAGCTATGCTGGAAACAGCATAGCAAGTTTAAATAAGGCTAGTCCGTTATCA ACTTGAAAAAGTGGCACCGAGTCGGTGCTTTTTTT-3′	Fig. 4f, ED 7
GAPDH-targeting sgRNA 4 T7 template†	5′-**GG**ATGTCATCATATTTGGCAGGGTTTAAGAGCTATGCTGGAAACAGCATAGCAAGTTTAAATAAGGCTAGTCCGTTATCA ACTTGAAAAAGTGGCACCGAGTCGGTGCTTTTTTT-3′	NA
GAPDH-targeting sgRNA 4	5′-**TAATACGACTCACTATAGG**ATGTCATCATATTTGGCAGGGTTTAAGAGCTATGCTGGAAACAGCATAGCAAGTTTAAAT AAGGCTAGTCCGTTATCAACTTGAAAAAGTGGCACCGAGTCGGTGCTTTTTTT-3′	Fig. 4f, ED 7
GAPDH PAMmer 1	5′-ATGACCCT**TGG**GGCTCCCCCCTGCAAA-3′	Fig. 4f,g, ED 7
GAPDH PAMmer 2	5′-TGGATGAC**CGG**GGCCAGGGGTGCTAAG-3′	Fig. 4f, ED 7
GAPDH PAMmer 3	5′-TTGGCAGG**TGG**TTCTAGACGGCAGGTC-3′	Fig. 4f, ED 7
GAPDH PAMmer 4	5′-CCCCAGCG**TGG**AAGGTGGAGGAGTGGG-3′	Fig. 4f, ED 7
GAPDH PAMmer 1 2′OMe v1‡	5′-A*UGACC*CTAGG*GGCTC*CCCCC*UGCAA*A-3′	Fig. 4g, ED 7
GAPDH PAMmer 1 2′OMe v2‡	5′-*ATG*ACC*CU*AGG*GGC*UCC*CCC*CTG*CAA*A-3′	Fig. 4g, ED 7
GAPDH PAMmer 1 2′OMe v3‡	5′-*ATG*ACCC*UAGG*GGCT*CCCC*CCTG*CAA*A-3′	Fig. 4g, ED 7
GAPDH PAMmer 1 2′OMe v4‡	5′-*AT*GA*CC*CT*AGG*GG*CT*CC*CC*CC*UG*CA*AA-3′	Fig. 4g, ED 7
GAPDH PAMmer 1 2′OMe v5‡	5′-*AT*GA*CC*CT*AG*GG*GC*TC*CC*CC*CU*GC*AA*A-3′	Fig. 4g, ED 7
GAPDH cDNA primer Fwd	5′-CTCACTGTTCTCTCCCTCCGC-3′	Fig. 4g,f, ED7
GAPDH cDNA primer Rev	5′-AGGGGTCTACATGGCAACTG-3′	Fig. 4g,f, ED7
β-actin cDNA primer Fwd	5′-AGAAAATCTGGCACCACACC-3′	Fig. 4g,f, ED7
β-actin cDNA primer Rev	5′-GGAGTACTTGCGCTCAGGAG-3′	Fig. 4g,f, ED7

* Guide crRNA sequences and complementary DNA target strand sequences are shown in red. PAM sites (5′-NGG-3′) are highlighted in yellow on the non-target strand when adjacent to the target sequence or in the PAMmer.
† The T7 promoter is indicated in bold (or reverse complement of), as well as 5′ G or GG included in the ssRNA product by T7 polymerase. sgRNAs for *GAPDH* were designed according to Chen *et al.*[32]
‡ Positions of 2′-OMe modifications depicted with asterisks preceding each modified nucleotide.
NA, not applicable.

©2014 Macmillan Publishers Limited. All rights reserved